de B. Hornibrook, in *Tertiary Correlations and Climatic Changes in the Pacific*, K. Hatai, Ed. (Sasaki, Sendai, Japan, 1966), p. 29.
17. T. Tanai and K. Huzioka, in *Tertiary Correlations and Climatic Changes in the Pacific*, K. Hatai, Ed. (Sasaki, Sendai, Japan, 1966), p. 89.
18. E. Dorf, *Geol. Soc. Amer. Spec. Pap. 62* (1955), p. 575.
19. J. A. Wolfe and D. M. Hopkins, in *Tertiary Correlations and Climatic Changes in the Pacific*, K. Hatai, Ed. (Sasaki, Sendai, Japan, 1966), p. 67.
20. U.S. Geological Survey collections, Menlo Park, California.
21. S. R. Capps, *U.S. Geol. Surv. Bull.* **880-C**, 111 (1937).
22. W. H. Dall and G. D. Harris, *U.S. Geol. Surv. Bull.* **84** (1892); W. H. Dall, *Harriman Alaska Exped.* **4**, 99 (1904).
23. D. J. Miller, *U.S. Geol. Surv. Map OM 187* (1957).
24. N. L. Taliaferro, *Bull. Geol. Soc. Amer.* **43**, 749 (1932).
25. D. J. Miller, *J. Geol.* **61**, 17 (1953).
26. D. W. Turner, thesis, University of California, Berkeley (1968).
27. J. C. Clark, thesis, Stanford University (1966).
28. C. E. Weaver *et al.*, *Bull. Geol. Soc. Amer.* **55**, 569 (1944).
29. C. M. Wagner and K. H. Schilling, *Univ. Calif. Publ. Geol. Sci.* **14**, 235 (1923); K. C. DeLise, *ibid.* **68** (1967); A. Clark, unpublished reports (University of California, Riverside).
30. W. Loel and W. H. Corey, *Univ. Calif. Publ. Geol. Sci.* **22**, 31 (1932).
31. W. O. Addicott, *U.S. Geol. Surv. Prof. Pap. 642*, in press.
32. H. M. Preston, *Calif. Oil Fields* **16**, 5 (1931); W. O. Addicott and J. G. Vedder, *U.S. Geol. Surv. Prof. Pap. 475-C* (1963), p. C63.
33. J. O. Nomland, *Univ. Calif. Publ. Geol. Sci.* **10**, 293 (1917); O. S. Adegoke, *Nautilus* **80**, 91 (1967).
34. J. O. Nomland, *Univ. Calif. Publ. Geol. Sci.* **10**, 191 (1917).
35. W. P. Woodring, R. B. Stewart, R. W. Richards, *U.S. Geol. Surv. Prof. Pap. 195* (1940).
36. R. M. Kleinpell and D. W. Weaver, *Univ. Calif. Publ. Geol. Sci.* **43** (1963).
37. University of California, Berkeley, locations A494-6, A499, La Panza Range, San Luis Obispo County, California.
38. F. M. Anderson and B. Martin, *Proc. Calif. Acad. Sci. Ser. 4* **4**, 15 (1914).
39. C. A. Hall, Jr., *Univ. Calif. Publ. Geol. Sci.* **34**, 281 (1960); W. P. Woodring, *U.S. Geol. Surv. Prof. Pap. 147-C* (1926), p. C25.
40. D. L. Durham and W. O. Addicott, *U.S. Geol. Surv. Prof. Pap. 524-A* (1965), p. A-1.
41. W. P. Woodring and M. N. Bramlette, *U.S. Geol. Surv. Prof. Pap. 222* (1950).
42. J. E. Allen, thesis, University of California, Berkeley (1945).
43. R. Arnold, *Proc. U.S. Nat. Mus.* **34**, 345 (1908).
44. O. E. Bowen, in *Symposium of Papers*, E. W. Rennie, Jr., Ed. (American Association of Petroleum Geologists, Pacific Section, Bakersfield, Calif., 1965).
45. W. O. Addicott, *Proc. Calif. Acad. Sci.*, in press.
46. H. E. Vokes, P. D. Snavely, Jr., D. A. Myers, *U.S. Geol. Surv. Map OM 110* (1951); C. J. Hickman, thesis, University of Oregon (1968).
47. H. E. Vokes, N. Norbisrath, P. D. Snavely, Jr., *U.S. Geol. Surv. Oil Gas Invest. Prelim. Map 88* (1949).
48. E. J. Moore, *U.S. Geol. Surv. Prof. Pap. 419* (1963); Newport embayment and Cape Kiwanda area.
49. *Molopophorus stephensoni* zone.
50. *Echinophoria rex* zone.
51. B. L. Clark and R. Arnold, *Univ. Calif. Publ. Geol. Sci.* **14**, 123 (1923).
52. W. H. Dall, *Amer. J. Sci.* **4**, 305 (1922).
53. C. E. Weaver, *Wash. Geol. Surv. Bull.* **15** (1916); University of Washington Sylvia Creek (location 68), Grays Harbor County, Washington.
54. A. B. Reagan, *Trans. Kans. Acad. Sci.* **22**, 131 (1909).
55. Publication authorized by the director, U.S. Geological Survey.

21 April 1969

Modified Spinel, Beta-Manganous Orthogermanate: Stability and Crystal Structure

Abstract. *A new high-pressure polymorph with a modified spinel structure, β-Mn_2GeO_4, is stable in a pressure range intermediate between the field of the polymorph with the olivine structure and that of another high-pressure polymorph. Oxygen atoms are located approximately in cubic close packing with manganese and germanium atoms in octahedral and tetrahedral interstices, respectively, as in the spinel structure; however, germanium atoms form Ge_2O_7 groups instead of isolated GeO_4 groups.*

High-pressure transformations in R_2MX_4 compounds (*1*) are important in the interpretation of the rapid increase of seismic velocity at a certain depth in the earth's mantle. The olivine-spinel transformation of R_2MX_4 compounds has been observed in Mg_2GeO_4, Fe_2SiO_4, Ni_2SiO_4, and Co_2SiO_4. Ringwood and Major (*2*) reported a noncubic high-pressure polymorph, a "distorted" or "modified" spinel, in transformations of $(Mg_{0.85}Fe_{0.15})_2SiO_4$ and Mg_2SiO_4. They considered that this high-pressure polymorph, β-Mg_2SiO_4, is produced from a true spinel when pressure is released. However, Ringwood's investigation (*3*) of the phase relations of the system Mg_2SiO_4-Fe_2SiO_4 at high pressures indicates that the β-phase is thermodynamically stable in its synthesis field. Akimoto and Sato (*4*) demonstrated that β-Co_2SiO_4, which is analogous to β-Mg_2SiO_4, is stable in a special field intermediate between the olivine and spinel fields.

In our study of the phase relations of Mn_2GeO_4, β-Mn_2GeO_4 was obtained. Because the β-phase is important in the high-pressure transformations of R_2MX_4 compounds, the stability field and crystal structure of β-Mn_2GeO_4 have been investigated.

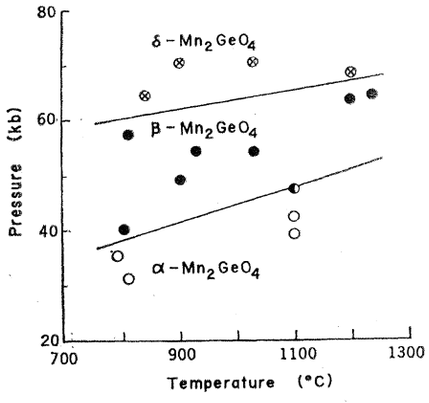

Fig. 1. Stability diagram for the high-pressure and high-temperature transformations of Mn_2GeO_4. Starting material is α-Mn_2GeO_4; ○, no change after runs; ● and ⊗, changes to β- and δ-Mn_2GeO_4, respectively, after runs.

Phase relations of Mn_2GeO_4 were studied from 790° to 1240°C in the pressure range 31 to 70 kb with the tetrahedral anvil type of high-pressure apparatus (*5*). The high-pressure polymorph β-Mn_2GeO_4 is stable in the pressure range intermediate between the fields of the olivine-type polymorph, α-Mn_2GeO_4, and another high-pressure polymorph, δ-Mn_2GeO_4 (Fig. 1) (*6*). In all experiments, α-Mn_2GeO_4 was used as the starting material. The cell dimensions, space groups, and densities of the three polymorphs are given in Table 1. A true spinel type, γ-phase, has not been observed in Mn_2GeO_4; the densest polymorph, δ-Mn_2GeO_4, has the Sr_2PbO_4-type structure in which Ge atoms are located in the octahedral interstices of oxygen atoms (*7*). The increases of density from α-Mn_2GeO_4 to β-Mn_2GeO_4 and from β-Mn_2GeO_4 to δ-Mn_2GeO_4 are 7.1 and 10.7 percent, respectively.

The structure of β-Mn_2GeO_4 has been determined from single crystals synthesized at 1240°C and 64 kb. The orthorhombic cell dimensions of β-Mn_2GeO_4 are comparable to those of β-Mg_2SiO_4 and β-Co_2SiO_4 (Table 2). The calculated density is 5.13 g cm^{-3} with eight formula units per cell. The diffraction pattern is *I--a*, which suggests the possible space groups *Imma*, *I2ma*, and *Im2a*. A nearly spherical crystal, 0.1 mm in diameter, was used for collecting the intensity data. Three-dimensional intensities for 521 symmetrically independent reflections were measured on an automatic four-circle diffractometer; molybdenum radiation was used out to a maximum diffraction angle of $2\theta = 60°$ by the $\omega - 2\theta$ scan method. The intensities were corrected for Lorentz and polarization factors. No absorption correction was made.

Because the unit cells of β-Mg_2SiO_4 and β-Co_2SiO_4 are obtained by the transformation matrix

$$\begin{bmatrix} \frac{1}{2} & \frac{\overline{1}}{2} & 0 \\ 1 & 1 & 0 \\ 0 & 0 & 1 \end{bmatrix}$$

from those of the corresponding true spinels, it is reasonable to assume that oxygen atoms occupy similar positions in both structures with cubic close packing. If we assume symmetry centers in the structure of the β-phase, the possible space group is *Imma*. The Patterson projection on (100) of β-Mn_2GeO_4 made possible a determination of the positions of metal atoms—tetrahedral sites (*A* sites) for Ge atoms and octahedral sites (*B* sites) for Mn atoms. The Fourier projections on (001) and (100) were synthesized to obtain the displacements of oxygen and metal atoms from the positions determined as above. Further refinements were carried out by the full-matrix, least-squares method (*8*). The residual *R* reduced to 0.057 for all 521 reflections and 0.051 for 490 observed reflections for the final structure (Table 3).

In the structure of β-Mn_2GeO_4 viewed in the [100] direction (Fig. 2), the oxygen atoms are approximately in cubic close packing as in the spinel structure. The Ge atoms occupy the *A* sites and the Mn atoms occupy the *B* sites. However, the arrangements of the *A* and *B* sites in β-Mn_2GeO_4 are different from those in spinel. For comparison, the structure of spinel with R_2MX_4 composition, where the *M* atoms are on the *A* sites and the *R* atoms are on the *B* sites, is shown in Fig. 3. Two GeO_4 tetrahedra, which would be isolated in the spinel structure, share one of their oxygen atoms and form a Ge_2O_7 group and an oxygen atom not bonded to any Ge atom. Thus the spinel structure must be modified by the displacement of four *M* and four *R* atoms out of the eight *M* and sixteen *R* atoms in the cell.

Table 1. Cell dimensions and corresponding standard deviations, space group, and density of Mn_2GeO_4 polymorphs. Radiation used was $CuK\alpha_1$ (1.5405 Å).

Polymorph	*a* (Å)	*b* (Å)	*c* (Å)	Space group	Density (g cm^{-3})
α-Mn_2GeO_4	5.061 ± 0.001	10.719 ± 0.001	6.295 ± 0.001	*Pbnm*	4.79
β-Mn_2GeO_4	6.025 ± 0.002	12.095 ± 0.004	8.752 ± 0.002	*Imma*	5.13
δ-Mn_2GeO_4	5.262 ± 0.001	9.274 ± 0.001	2.954 ± 0.001	*Pbam*	5.68

Table 2. Cell dimensions and corresponding standard deviations of the β-phases for three compositions.

Composition	*a* (Å)	*b* (Å)	*c* (Å)
Mg_2SiO_4 (*2, 4*)	5.710 ± 0.004	11.45 ± 0.02	8.248 ± 0.009
Co_2SiO_4 (*4*)	5.753 ± 0.001	11.522 ± 0.004	8.337 ± 0.002
Mn_2GeO_4	6.025 ± 0.002	12.095 ± 0.004	8.752 ± 0.002

Table 3. Atomic coordinates (expressed in cell edges) and isotropic temperature factors of β-Mn_2GeO_4 and corresponding standard deviations.

Atom	Atomic coordinates			Isotropic temperature *B* (Å^2)
	x	*y*	*z*	
Mn(1)	0.0000	0.0000	0.0000	0.49 ± 0.06
Mn(2)	.0000	.2500	−0.0319 ± 0.0003	0.43 ± 0.05
Mn(3)	.2500	.1281 ± 0.0002	.2500	0.49 ± 0.03
Ge	.0000	.1193 ± 0.0001	.6165 ± 0.0002	0.37 ± 0.02
O(1)	.0000	.2500	.2123 ± 0.0013	0.80 ± 0.23
O(2)	.0000	.2500	.7191 ± 0.0014	1.10 ± 0.25
O(3)	.0000	−0.0088 ± 0.0007	.2546 ± 0.0012	0.89 ± 0.18
O(4)	.2586 ± 0.0009	.1224 ± 0.0008	−0.0033 ± 0.0006	0.94 ± 0.09

The O(1) is not bonded to any Ge atom but is bonded to five Mn atoms; O(2) is bonded to two Ge atoms and one Mn atom, because of the formation of the Ge_2O_7 groups; O(3) and O(4) are bonded to one Ge atom and three Mn atoms. The Ge-O distances of the tetrahedra range from 1.749 to 1.818 Å with a mean value of 1.772 Å; the Mn-O distances of the octahedra range from 2.133 to 2.239 Å with a mean value of 2.188 Å. Pauling's electrostatic balance rule fails for O(1) and O(2), the charge balance being $-\frac{1}{3}$ for O(1) and $+\frac{1}{3}$ for O(2).

If we may assume spinel structure for Mn_2GeO_4, we can deduce a value of 0.369 for the *x* coordinate of the oxygen atoms on the assumption that the Ge-O and Mn-O distances are the

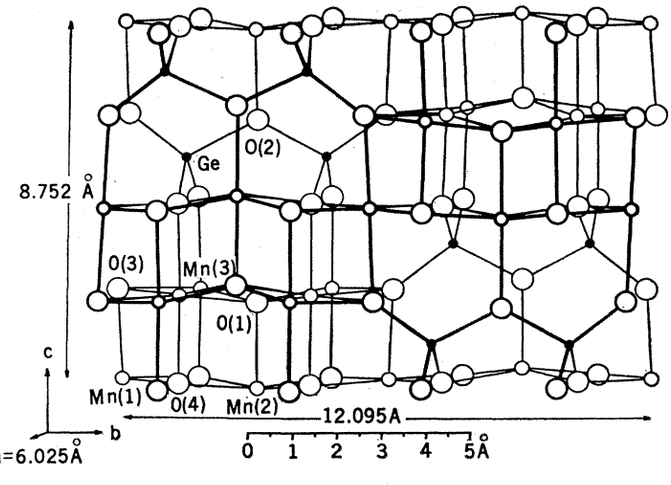

Fig. 2 (left). Orthorhombic crystal structure of β-Mn_2GeO_4.

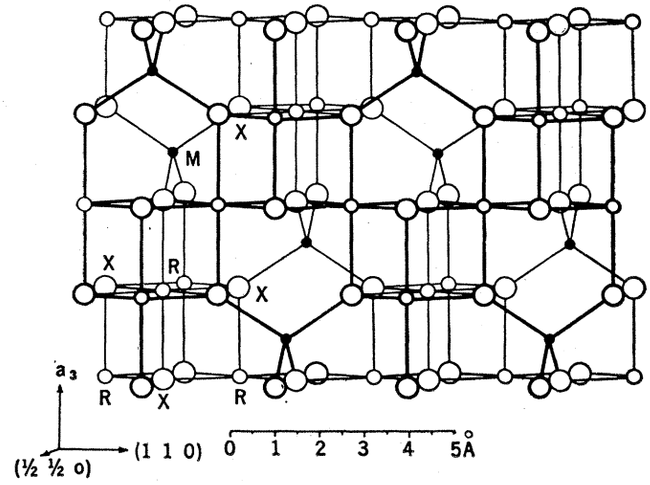

Fig. 3 (right). Cubic crystal structure of spinel, R_2MX_4.

same as in the β-phase. In this structure, the shared edges (3.16 Å) are longer than the unshared edges (3.02 Å) for the Mn octahedra. However, for β-Mn_2GeO_4, the shared edges (3.06 Å on the average) are shorter than the unshared edges (3.12 Å on the average). Because a shortening of the shared polyhedral edges is an important stabilizing factor for the ionic crystals (*9*), the stability of the β-phase in Mn_2GeO_4 might be explained by this shortening.

NOBUO MORIMOTO
Institute of Scientific and Industrial Research, Osaka University, Yamadakami, Suita, Osaka, Japan
SYUN-ITI AKIMOTO
Institute for Solid State Physics, University of Tokyo, Roppongi, Minato, Tokyo, Japan
KICHIRO KOTO
MASAYASU TOKONAMI
Institute of Scientific and Industrial Research, Osaka University

References and Notes

1. W. G. Wyckoff, *Crystal Structures* (Interscience, New York, ed. 2, 1965), vol. 3, pp. 75–83.
2. A. E. Ringwood and A. Major, *Earth Planet. Sci. Lett.* **1**, 241 (1966).
3. A. E. Ringwood, *Australian Nat. Univ. Dep. Geophys. Geochem. Publication No. 666* (1969).
4. S. Akimoto and Y. Sato, *Tech. Rep. Inst. Solid State Phys. Univ. Tokyo Ser. A No. 328* (1968).
5. S. Akimoto, H. Fujisawa, T. Katsura, *J. Geophys. Res.* **70**, 1969 (1965).
6. We refer to the polymorphs of the R_2MX_4 compounds as follows: α-phase (olivine type); β-phase (modified spinel type); γ-phase (spinel type); and δ-phase (Sb_2PbO_4 type). This decision was made at a meeting of S. Akimoto, N. Kawai, P. Moore, N. Morimoto, A. E. Ringwood, and T. Takahashi held at the Department of Geophysics and Geochemistry, Australian National University, Canberra, January 1969.
7. A. D. Wadsley, A. F. Reid, A. E. Ringwood, *Acta Crystallogr.* **B24**, 740 (1968).
8. W. R. Busing, K. O. Martin, H. A. Levy, *U.S. At. Energy Comm. Res. Develop. Rep. ORNL-TM-305* (1962).
9. L. Pauling, *The Nature of the Chemical Bond* (Cornell Univ. Press, Ithaca, N.Y., ed. 3, 1960), p. 559; B. Kamb, *Amer. Mineral.* **53**, 1439 (1968).
10. We thank Dr. J. D. H. Donnay for reviewing the manuscript and making suggestions for improvement.

23 December 1968; revised 15 April 1969

Visual Transient Phenomenon: Its Polarity and a Paradox

Abstract. *Luminance stimuli modulated at frequencies above flicker fusion create perceptible visual transient responses when the frequency is changed abruptly. The polarity of these transients, as directly perceived and objectively confirmed, is shown enough by itself to yield a powerful criterion for visual models. An apparent paradox when light flashes are superposed on the frequency discontinuity has further implications for models and suggests a possible nonconservation of polarity in the brightness perception process.*

A light whose luminance oscillates rapidly enough around a constant level $\bar{L}$ is seen as the unvarying luminance $\bar{L}$ (Talbot-Plateau law), provided among other things the frequency is constant. Flicker can be sensed, however, even with oscillations always faster than fusion and $\bar{L}$ kept constant, if the frequency itself is modulated by abruptly alternating increases and decreases (*1*). Not surprisingly, the alternation rate must be below fusion (*2*). Of great interest, however, is the fact that the eye does respond to the individual frequency jumps (*3*). We are studying that elemental response and discuss here its curious nature.

The stimulus studied (Fig. 1) contains one abrupt frequency change, with both periods t_1 and t_2 shorter than the fusion limit, and both wavetrains long enough to insure that the eye is in a steady-state at the time of the period discontinuity and is unperturbed by the stimulus cutoff. When one views this stimulus, a transient effect is experienced at the jump in period if $|t_2 - t_1|$ is large enough (*3*). For example, with a moderately high mean luminance $\bar{L}$, the effect is readily apparent for the case $t_1 = 1$ msec and $t_2 = 5$ msec.

These transients have an interesting appearance. Careful observers agree that with t_1 less than t_2 as depicted in Fig. 1, the period jump is perceived as a brief eclipse, whereas, with the reverse configuration t_1 greater than t_2, the experience is a momentary increase in brightness. That period discontinuities are perceived as brightness changes is interesting, but understandable (see Eq. 5). Also, details of the thresholds, reaction times, $\bar{L}$ dependence, and so forth no doubt contain a wealth of information on the temporal sensitivity of the eye. However, we focus here on just the polarity of the transients, for it alone is very significant.

In reporting (*4*) on the polarity of the transient, we described some objective tests (thresholds and reaction times) which confirm the direct perception. If, as is natural with luminance increases taken as positive, we assign positive sign to brightness increments and negative to decrements, the observed polarity is summed up by

$$\text{sign of transient} = \text{sign of } [t_1 - t_2] \quad (1)$$

This property is readily reconciled with only one of the deLange-Kelly class of visual models (*4*). Here we shall generalize that result, deducing from Eq. 1 a stringent criterion applicable to many different models.

An apparent paradox was also noted on adding a short flash simultaneous with the period jump (*4*)—the percept is diminished by a flash of the same sign as the transient alone (Eq. 1), and is enhanced by a flash of opposite sign. The paradox is highlighted by related studies which deduced incorrectly a sign for the transients (*5*). One simple and plausible way it might be resolved (*4*) is extended below to general linear theories.

Turning now to visual models, let us require that they reproduce the observed polarity and the apparent paradox. For brightness perception at high frequencies, deLange (*6*) has argued in favor of linear models. For these, or for the linear limit of a nonlinear model, we can easily demonstrate how severe our requirements can be.

Consider any linear model whose response, subject to some detection rule, is to be a brightness analog. The response $R(t)$ to an input $I(t)$ may be expressed in general as (*7*)

$$R(t) = \int_{-\infty}^{\infty} G(t,t')\, I(t')\, dt' \quad (2)$$

where the Green's function $G(t,t')$ is the response to an impulse $\delta(t-t')$, which completely specifies the model. For the input discontinuous at $t=0$ (Fig. 1) we write

$$I(t) = I_1(t) + S(t)\,[I_2(t) - I_1(t)] \quad (3)$$

where the unit step $S(t) = \int_{-\infty}^{t} \delta(t')dt'$. Inserting Eq. 3 into Eq. 2 and using causality ($G(t,t') = 0$ for $t < t'$) gives $R = \int_{-\infty}^{\infty} G\, I_1$ for $t < 0$ and $R = \int_{-\infty}^{\infty} G\, I_2 + \int_{-\infty}^{0} G[I_1 - I_2]$ for $t > 0$. Now if I_1 and I_2 oscillate rapidly about the same mean $\bar{I}$ and if we require the model to satisfy the Talbot-Plateau law above, then $\int_{-\infty}^{\infty} GI_1 = \int_{-\infty}^{\infty} GI_2 \propto \bar{I}$ within undetected fluctuations. Therefore we obtain the

$$\text{transient} = S(t) \int_{-\infty}^{0} G(t,t')\,[I_1(t') - I_2(t')]\, dt' \quad (4)$$